Scientific Research Publishing

Advances in Chemical Engineering and Science, 2026, 16(4), 139-158
https://www.scirp.org/journal/aces
ISSN Online: 2160-0406
ISSN Print: 2160-0392

Refractometric Determination of Thermodynamic Hydrate Inhibitor Concentrations under Variable Operating Conditions: A Physicochemical Evaluation

Tombari Ransome Mbooh[1*], Ogbonna Friday Joel[2], Nuka Dumle Nwiabu[3], Joe Emmanuel Akhagbeme[2]

[1]World Bank Africa Centre of Excellence for Oil Field Chemical Research, University of Port Harcourt, Port Harcourt, Nigeria
[2]Department of Petroleum and Gas Engineering, University of Port Harcourt, Port Harcourt, Nigeria
[3]Department of Computer Science, Rivers State University, Port Harcourt, Nigeria

Email: *mbooh.tombari@aceceforuniport.edu.ng, ogbonna.jeol@uniport.edu.ng, nwiabu.nuka@ust.edu.ng, joe_akhagbeme@uniport.edu.ng

How to cite this paper: Mbooh, T.R., Joel, O.F., Nwiabu, N.D. and Akhagbeme, J.E. (2026) Refractometric Determination of Thermodynamic Hydrate Inhibitor Concentrations under Variable Operating Conditions: A Physicochemical Evaluation. *Advances in Chemical Engineering and Science*, **16**, 139-158.
https://doi.org/10.4236/aces.2026.164007

Received: March 6, 2026
Accepted: August 31, 2026
Published: September 3, 2026

Abstract

Accurate optimization of hydrate inhibition requires knowledge of the actual inhibitor concentration retained in the aqueous phase under operating conditions. This study applied refractometry to determine effective concentrations of monoethylene glycol (MEG) and methanol (MeOH). Calibration curves were developed using known weight-percent solutions, yielding strong correlations between refractive index and concentration ($R^2 > 0.98$). Samples extracted from a mini-hydrate flow loop at varying pressures confirmed a linear relationship between the input dosage and the actual concentration ($R^2 > 0.99$). MEG retained ~95% of its input dosage, while MeOH retained ~90%. Concentrations decreased slightly with lower operating pressures, reflecting volatility and gas-phase partitioning effects. These findings demonstrate refractometry as a reliable, cost-effective method for real-time monitoring and optimization of hydrate inhibitors.

Keywords

Gas Hydrate, Refractive Index Measurement, Hydrate Inhibitors Optimization, Inhibitor Actual Concentration, Flow Assurance

1. Introduction

The transportation or delivery of oil and gas in environments characterized by

low temperatures, high pressures, and high-water cuts poses a significant risk of hydrate formation [1]. According to Koh, water and gas molecules combine under such conditions to form hydrates. These hydrates are similar to ice in terms of their physical properties [2]. They are about 85% water molecules and 15% gas molecules (by mole ratio). However, no chemical reaction occurs between the constituent molecules; rather, the gas molecules are trapped within a crystalline water lattice. Gas hydrate, commonly referred to simply as hydrate, is a substance composed of water and gas. It's best characterized as a non-stoichiometric, crystalline, and clathrate compound with a regular repeating internal structure consisting of hollow units (cavities, or cages) in which the guest and the host molecules do not have a fixed ratio [3]. This structural character in hydrates is attributable to hydrogen bonding between water molecules. If gas molecules become trapped in these cages, you get hydrates. In such a situation, the water, or in general, the hosts (guest molecules or solute), play their roles and are balanced against geometric elements—products themselves of the molar ratio. The typical guest molecules are methane, ethane, propane, butane, carbon dioxide, hydrogen sulfide, and even nitrogen [4]. Hydrates are divided into three principal structural variants: Structure I, Structure II, and H, depending on the size and geometry of their cavities and the nature of guest gas molecules [5]-[7]. Gas hydrate formation poses significant risks in oil and gas transportation under low-temperature, high-pressure, and high-water-cut conditions. Hydrates are crystalline clathrate compounds composed of water and guest molecules (e.g., methane, ethane, CO_2), stabilized by hydrogen bonding. Their formation can obstruct flowlines, cause pressure buildup, and lead to costly production interruptions. Offshore operations cost may account for up to 8% of operating expenditure on hydrate prevention [8]. Therefore, finding the optimum weight percent of inhibitors is important to prevent hydrate formation effectively and economically. Those hydrates can also plug the flowlines and risers, thus limiting or even stopping gas production, and cause not only pressure accumulation but also lead to flow breakdown [9] [10]. Furthermore, hydrate-related problems have been encountered during drilling through HBS, resulting in borehole instability and gas kicks [11]. In some situations, hydrate plugs have stopped production for several days, due to safety, equipment damage, and revenue loss concerns [12]. Several techniques have been applied to design for hydrate-related events: depressurization, thermal insulation, passive, and active heating, electrical heating systems (tubing bundles with heat tracing), surface coatings, and coated flowlines [13]. Chemical injection for both in-block and out-of-block subsea well production systems, injection of hot water or oil through the flowlines to ensure lower intervention time during blockage caused by hydrates or waxes, pipeline inspection gauges (PIGs), etc. Of these, chemical injection appears to be the most cost-effective option, especially in an offshore environment where platform space is smaller, water depths are deeper, and production rates are high [14]-[16]. The chemicals that prevent hydrates from forming are called hydrate inhibitors. These inhibitors either inhibit hydrate formation or cause already formed hydrates to

dissolve. Generally, hydrate inhibitors are divided into two types: THIs and LDHIs [17] [18]. This effect is caused by changes in pressure and temperature in hydrate formation. This modification is achieved by breaking the hydrogen-bonding network of the hydrate system, resulting in a soft, structurally and thermodynamically unstable system [19]. As a result, hydrate may also be dense or unable to form under the initial formation environment [20]. In other words, the THIs places the hydrate formation boundary at more extreme conditions than at lower temperatures and/or higher pressures where hydrate formation is not favorable [21] [22].

There are two main types of LDHIs: these are Kinetic Hydrate Inhibitors (KHIs) and Anti-Agglomerate (AA) inhibitors. These inhibitors inhibit hydrate formation by affecting the action of the main factors, for example, low temperature, high pressure, and water [23]. KHIs are copolymers or homopolymers that are low molecular weight and soluble in water, based on cyclic amide (lactam) groups as active material [24]. Nevertheless, not all KHIs are polymers described by [25]; in some cases, they require application in a mixture formulation. KHIs work by inhibiting hydrate crystal initiation (or delaying the nucleation process) and thus extending the induction time. The waiting period before a solid hydrate crystal will occur. On the other hand, inhibitors that act against agglomerate formation by lowering the capillary forces (VDW interactions) between hydrate particles, preventing them from sticking together into larger masses [26]. Those inhibitors contact the liquid hydrocarbon phase to disperse the free water into fine droplets, inhibiting aggregation and growth of the hydrate nucleus [27]. The effectiveness of AA inhibitors is highly dependent on the type and nature of the surrounding liquid environment [28]. Regardless of the type used, the primary objective of hydrate inhibitors is to ensure the safe and cost-effective transportation of hydrocarbons. However, hydrate inhibitors are expensive, volatile, and toxic, depending on the type [29] [30]. Accordingly, it is crucial to determine the minimum effective weight percentage for hydrate inhibition at varying times. Overdoses can result in a waste of capital and operational expenditures. Underdosing may cause incomplete inhibition, thereby exacerbating the issue of hydrate-induced problems [31]. As emphasized by [31], there is a critical need to determine the optimum inhibitor concentration or injection rate under varying operational conditions—one that is sufficient to prevent hydrate formation without incurring excess cost. The reason for overdosing is to prevent the risk of hydrate formation and handle the event of an increase in water production, unexpected changes, and equipment breakdown. However, the issue of both overdosing and underdosing is being addressed by evaluating the actual weight percent of inhibitor in the system. Fluid samples collected downstream in the pipelines or separator are analyzed to account for the inhibitor weight percent. The lack of accurate information on the actual inhibitor weight percent. Knowing the inhibitor weight percent in the aqueous phase is then used to optimize, monitor, and prevent the risk of hydrate formation under control. Different techniques have been used to account for the actual weight percentage of inhibitors in the aqueous phase for hydrate optimization and monitoring.

The freezing point depression method was reported to have been used to analyze the concentration of the inhibitor [32]. Water activity, water content, and speed of sound techniques have been used by various researchers to evaluate inhibitors or salt concentration in aqueous solution [33] [34]. The electrical conductivity-velocity method was reported to be used by Mazloum, Yang, Chapoy & Tohidi, to account for the volume of inhibitor presence in the aqueous phase; however, the availability of ions in its solution remained a key issue [35]. Recently, spectroscopy has also been used to evaluate hydrate concentration (weight percent) with positive outcomes [36] [37].

Mitigation strategies include depressurization, thermal insulation, active heating, and chemical injection. Chemical inhibitors remain the most cost-effective option in offshore environments. Hydrate inhibitors are classified into thermodynamic inhibitors (THIS) and low-dosage hydrate inhibitors (LDHIs), which include kinetic hydrate inhibitors (KHIs) and anti-agglomerates (AAs). Effective inhibitors are costly and may pose environmental risks, therefore necessitating dosage optimization. Existing concentration determination methods, such as freezing point depression, conductivity, and spectroscopy, often suffer from high error margins or sensitivity to impurities. Refractometry offers a simple, accurate alternative, with reported errors as low as 3.1% [38].

This study investigates refractometry for determining actual MEG and MeOH concentrations under hydrate-forming conditions in a controlled flow loop.

Refractive index concept

When light travels through a material, it tends to interact with the component; this interaction can be made visible through its change or bend at the boundary (interface) of the two materials (media). Light refraction happened as a result of changes in the speed of the light wave. Light refraction may be considered the changing of light speed at the interface of two different materials as it passes from one material to another. The difficulty with which light rays pass through a material is captured via its optical density, which is expressed numerically in terms of refractive index. According to Worsfold, Townshend & Poole, the measurement of refractive index is referred to as refractometry. Refractometry is a technique used to determine a material's composition and/or structure by refractive index [39].

A less dense material has less difficulty than a denser material. Meaning a denser material causes light rays to travel more slowly (having less speed). The material molecules of the medium cause a time lag in the transportation of the light wave through it. Refractive index is used to compare the speed of light in a material to that of a vacuum. Every material in a pure state has a defined refractive index. Refractive index (Rd) is the ratio of the speed of light in a vacuum to that of a material, expressed as (Rd = c/v). Refractive index has been reported to be influenced by the density of material, which is affected by composition, temperature, and weight percent of solute [40]. This technique is used in the chemical, food, and pharmaceutical industries for evaluating product weight percentages. This technique is

commonly used for testing product purity and monitoring the formation. As the weight percent of solute in the solution increased, the density also increased, and it was reported that the relationship between refractive index and solute weight percent is linear [41].

2. Materials and Methods

Mini hydrate flow loop (as shown in Figure 1), refractometer, mono ethylene glycol (MEG), methanol (MeOH), water, plastic dropper, and compressed natural gas (CNG) with a specific gravity of 0.5, composed of 98.4 mol% of methane and 1.6 mol% carbon dioxide.

Experimental Setup

A locally fabricated mini hydrate flow loop [42] was employed to simulate offshore pipeline conditions. The system comprised 0.5-inch stainless steel tubing within PVC insulation, operating up to 500 psi and 30˚C, with a total length of 12 m. Components included pumps, control valves, a cooling unit, a mixing vessel, and instrumentation for pressure and temperature monitoring.

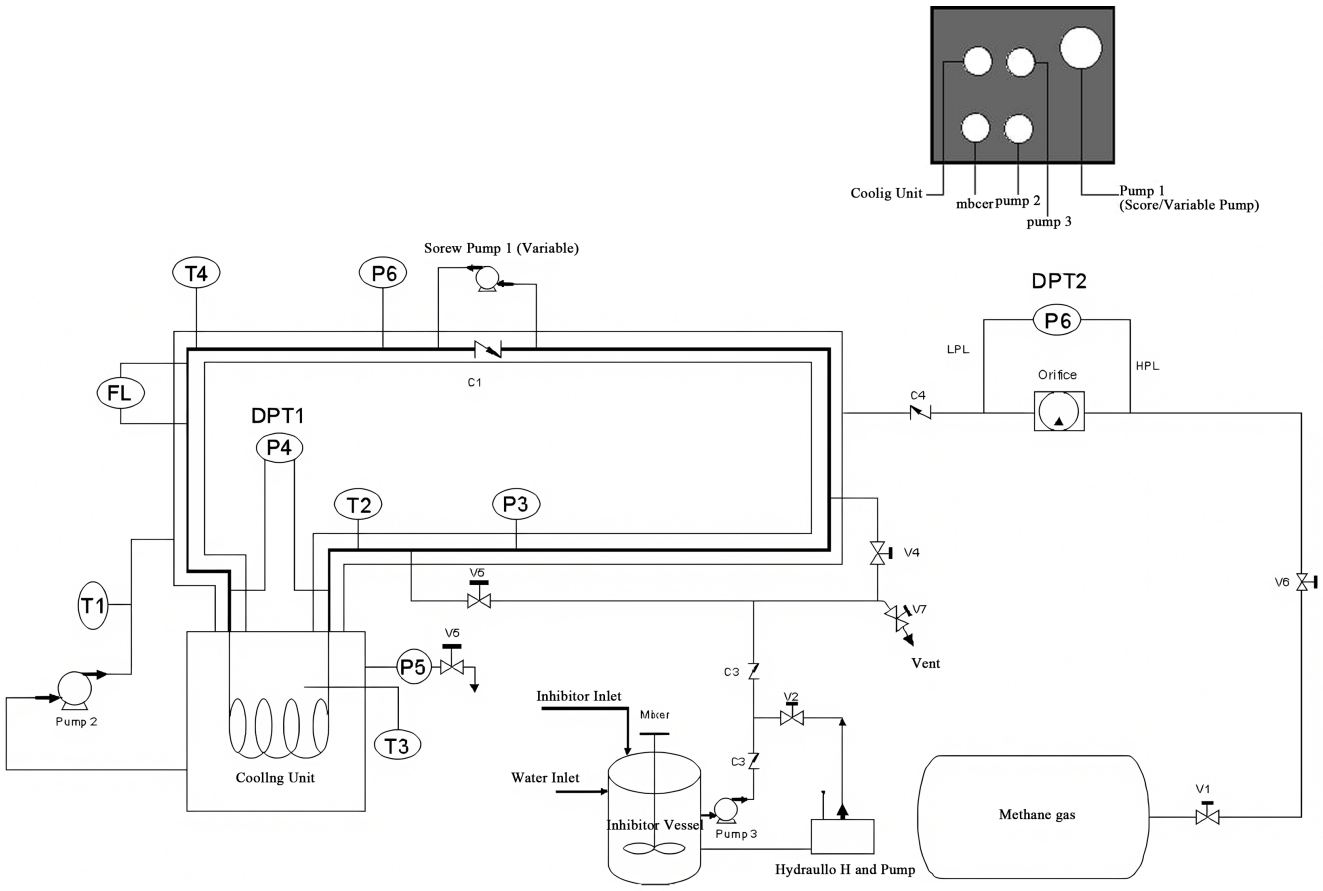

Figure 1. Process flow diagram for the mini hydrate flow loop [42].

3. Experimental Procedure

The details of the mini loop may be seen in [42]. The loop was used to condition

samples under different conditions. Before the commencement of the experiment, the mini flow loop was cleared with fresh water to remove any debris from the 0.5-inch tubing line. The entire loop was function-tested to check for leakages. Verify the control valves' alignment for proper isolation, confirm the responsiveness of control panel buttons, and perform zero-error checks on all measuring gauges. All the loop components were confirmed to be in proper working condition.

For each experimental run, 3000 ml of liquid (water and inhibitor) was measured and poured into the mixing vessel. With the power supply on and Pump 3 activated, the liquid was transferred from the mixing vessel into the 0.5-inch tubing. Once the vessel was emptied and a pressure of 25 psi was achieved, Pump 3 was turned off, and Valve 1 was opened to allow CNG into the system. The CNG was introduced until a pressure of 150 psi was attained, after which it was isolated from the loop. Pump 2 was then activated to circulate the liquid throughout the tubing. Water from the cooling unit was circulated through a PVC pipe using Pump 2, in a counter-current flow relative to the tubing to bring the loop to a low temperature. A reference test was conducted in the absence of any inhibitor, just water and gas from an initial 150 psi and 30˚C, for 120 minutes to evaluate the loop behaviour under hydrate-forming conditions. Pressure and temperature readings were taken at 2-minute intervals. This procedure was observed using the MEG system. The experiment was carried out at an initial pressure condition of 150 psi and a temperature of 30˚C. The following weight percent of samples (2 wt% to 18 wt% in increments of 2 wt%) and for each experiment run, the sample was taken at target operating pressures of 135 psi,130 psi, 125 psi,120 psi, and 115 psi, along with their respective temperature. The same set of experiments was conducted for MeOH. At each targeted pressure, the loop was put-off and flushed for about 2 minutes to free gas before samples were collected. 200 ml was taken for each sample, while the remaining volume was drained out. The loop was then flushed with fresh water and restored to its baseline conditions to eliminate memory effects and ensure the integrity of subsequent tests.

A refractometer was used to measure and calibrate the refractive indices of MEG and MeOH of the different weight percentages (2 wt% to 20 wt%). Distilled water was used to calibrate the refractometer (given a refractive index of 1.333) before the refractive measurement. For each measurement, the refractometer was left for 2 minutes after loading the sample to attain equilibrium. Again, the light was always adjusted, ensuring it pointed toward the middle of the crosshairs before taking the refractive reading. For all calibrated solutions, the refractometer was set at 20^0C. After each test, the prism was cleaned and allowed to dry for about 2 minutes before proceeding with the next run.

Each measurement was taken three times, with the average refractive index recorded. The refractive indices of samples extracted at different weight-percent inputs and operating pressures were measured at their respective extracted. Prior to each sample extraction the loop was opened for minutes until the samples free of

gas before collection. Clear and sealed sampling container were used for the sampled collection. Again, at point of refractive index measured, the samples were gently in-between the prims to avoid air bubbles.

4. Results and Discussion

Experimental data from refractive index measurements of known weight percentages for both MEG and MeOH were used to make various calibration plots. The relationship between refractive index and weight percent was analyzed with these plots via regression to evaluate the actual weight percent under different operating conditions.

Hydrate formation Result

Hydrate formation was monitored with a reference test, which was carried out in the absence of any inhibitor just water and gas under hydrate flow condition.

The gradual and continuous decrease in pressure confirmed hydrate formation. Pressure-decrease signal: gas withdrawal from the loop for hydrate formation. As seen in Figure 2, the pressure drops from 150 psi to 35 psi within 120 minutes in a gradual manner. Again, temperature increase was observed intermittently, indicating an exothermic process that was associated with hydrate formation. The results were in agreement with previous investigations with the loop [15] [22].

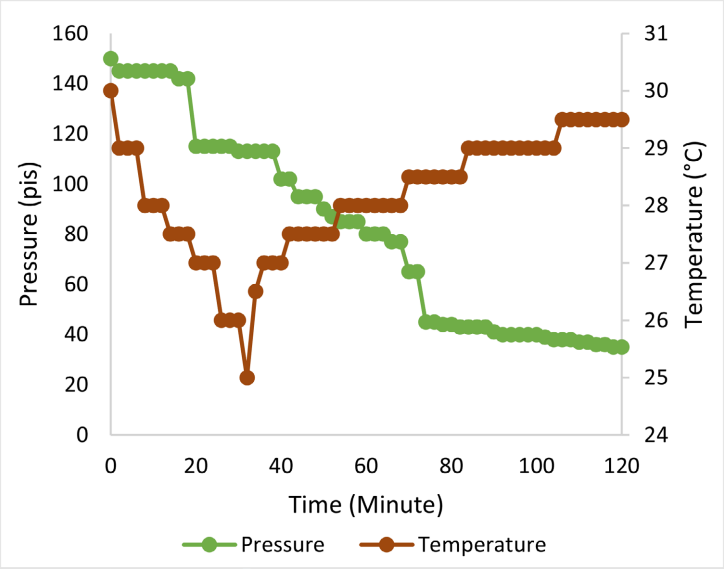

Figure 2. Pressure & temperature against time for reference test.

Inhibition Curve Results

The effectiveness of each weight percent for both inhibitors could be understand using the pressure, temperature, and time trends (P-T-t curve). Figures 3-7 showed the trend of pressure from initial tested pressure of 150 psi to 115 psi with their corresponding time and temperature. Averagely, an increased in the inhibitor concentration (weight percent) for both inhibitors from 2 wt% to 18 wt% increased the inhibition effectiveness, as higher concentration reduced the pres-

sure drop at a lower temperature, thereby elongating the time taking to reach the 115 psi mark. In another word, lower concentration witnessed fast pressure drop which is an indication of low inhibition effect [22]. MEG relatively at given a concentration showed superior performance when compared to MeOH.

As seen in Figures 3-7, pressure and temperature varies across each concentration, and the isolation of pressure effect from temperature effect was not feasible, this was due to the fact that hydrate or inhibition effect in term of pressure or pressure drop correspondent could only be achieved with loop temperature. Hence the pressure trend observed in each concentration should interpreted with respect time.

Calibration Curve Results

The calibration curves for both MeOH and MEG systems demonstrated a strong linear correlation between refractive index (Rd) and inhibitor weight percent across the range of 2 wt% to 20 wt% with all calibrated samples were measured

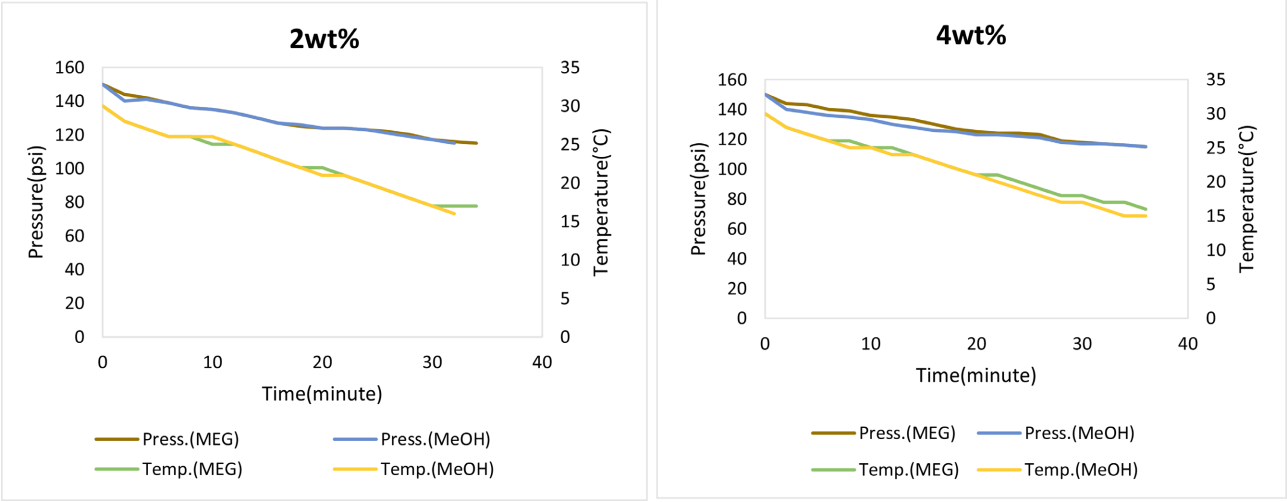

Figure 3. P-T-t curve for 2 wt% and 4 wt% of MEG and MeOH.

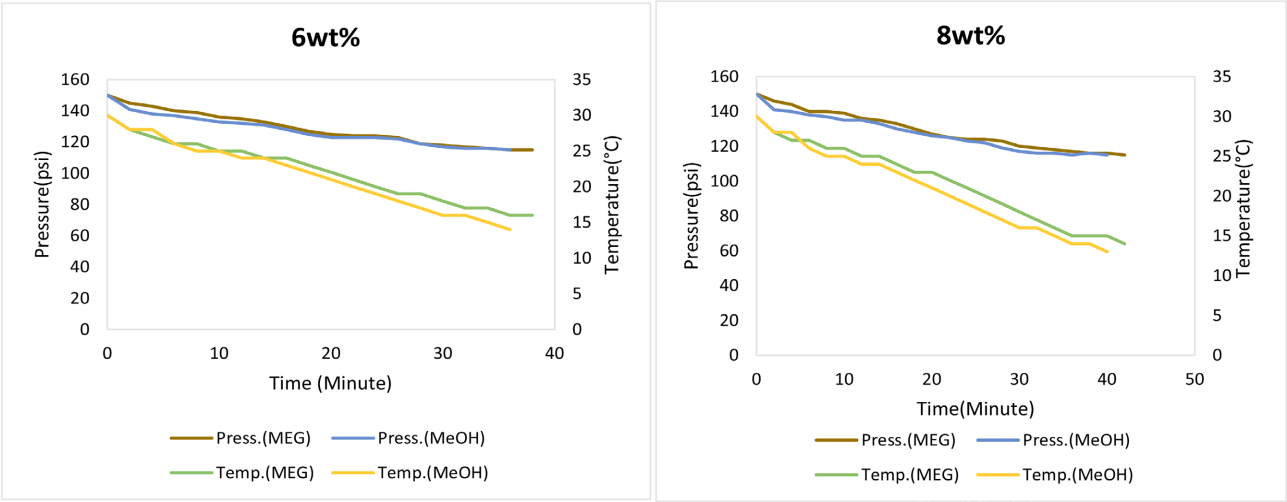

Figure 4. P-T-t curve for 6 wt% and 8 wt% of MEG and MeOH.

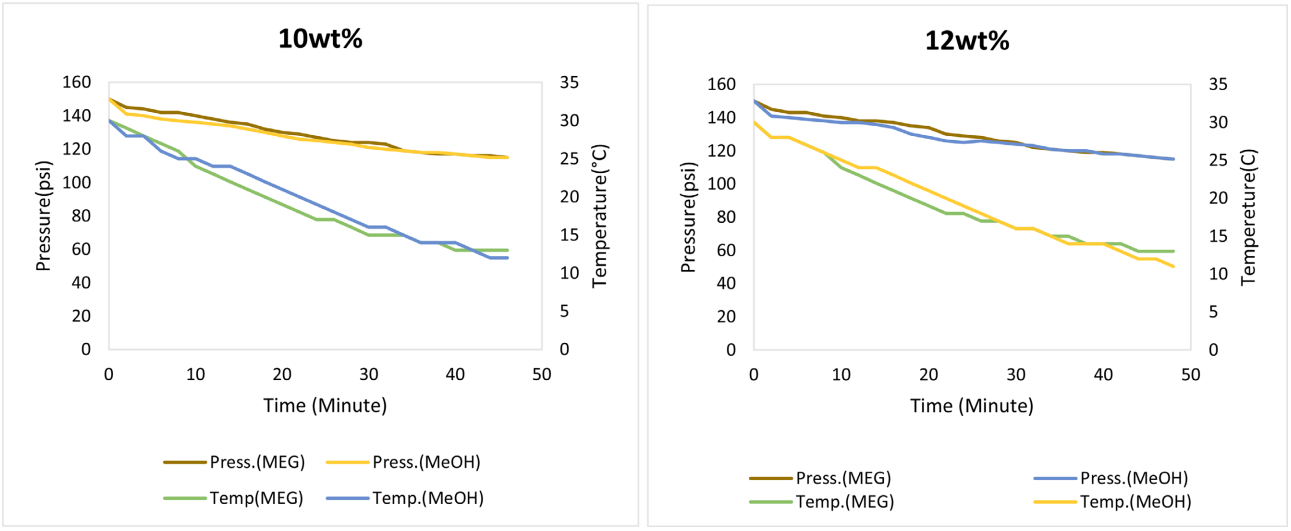

Figure 5. P-T-t curve for 10 wt% and 12 wt% of MEG and MeOH.

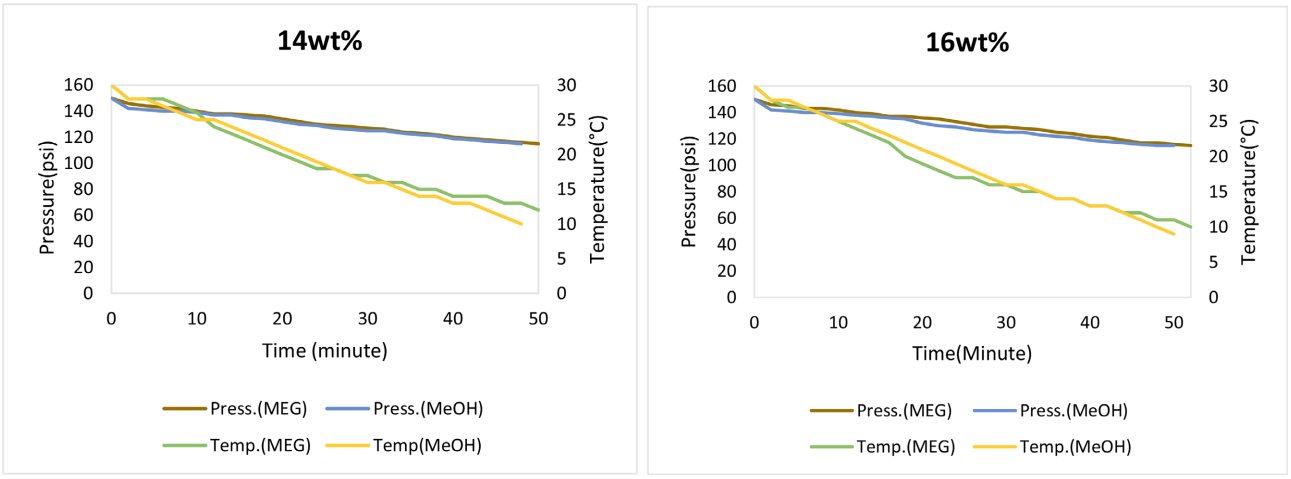

Figure 6. P-T-t curve for 14 wt% and 16 wt% of MEG and MeOH.

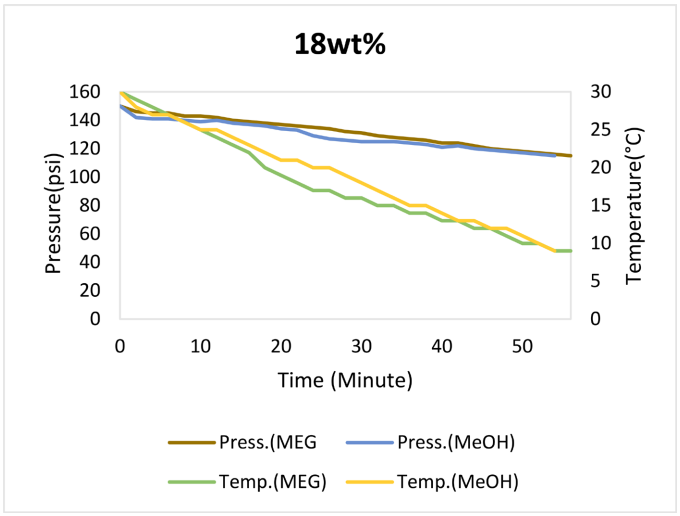

Figure 7. P-T-t curve for 18 wt% of MEG and MeOH.

at 20˚C. This correlation confirms that refractometry is a reliable method for quantifying inhibitor concentrations under hydrate-forming conditions. As the inhibitor concentration increased, the refractive index also increased, reflecting enhanced solution density and stronger molecular interactions [38].

For the MeOH system, refractive index values increased from 1.3336 at 2 wt% to 1.3401 at 20 wt%. In comparison, the MEG system showed a corresponding increase from 1.3413 at 2 wt% to 1.3579 at 20 wt% as seen in **Figure 8(a)** and **Figure 8(b)**. The higher refractive index values observed for MEG at equivalent weight percentages are attributed to its greater molecular weight and stronger hydrogen-bonding capacity, which result in denser solutions and more pronounced optical responses [29].

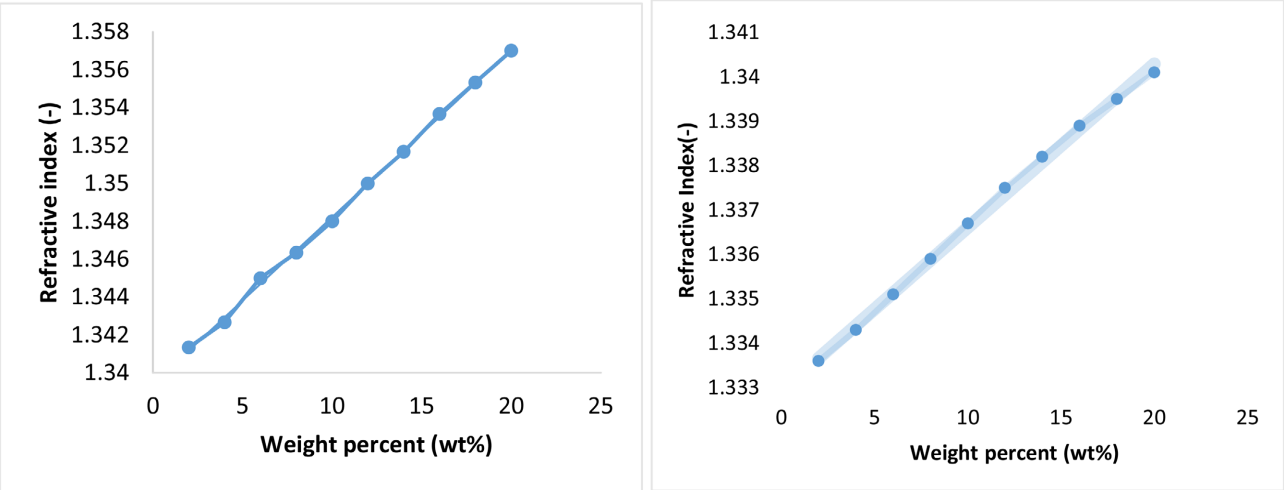

Figure 8. Relationship between Refractive index and Weight percent of MEG and MeOH.

These findings are consistent with previous studies that highlight MEG's superior stability and refractive sensitivity compared to MeOH, making it particularly suitable for refractometry-based monitoring of hydrate inhibition systems [18] [21].

Regression Analysis of Refractive Index and Weight Percent Relationship

Figure 9 showed the uncertainty analysis using error bar of the calibrated curve ranged from 2 wt% to 20wt for both inhibitors.

A linear regression analysis was carried out to establish the relationship between inhibitor weight percent (wt%) and refractive index (Rd) of both inhibitors (MEG and MeOH). The calibration data have good linearity for MeOH and MEG systems, demonstrating the reliability of the refractive index to predict inhibitor weight percent within the experimental range of 2 wt% - 20 wt%. The regressions obtained are as follows in **Table 1**, where: Rd = refractive index (dimensionless), C = weight percent (wt%).

Regression analysis indicated that both MeOH and MEG systems have a strong positive linear correlation of refractive index and weight percent, with $R^2 > 0.98$. The remaining slope values are different from the two inhibitors, which reflects

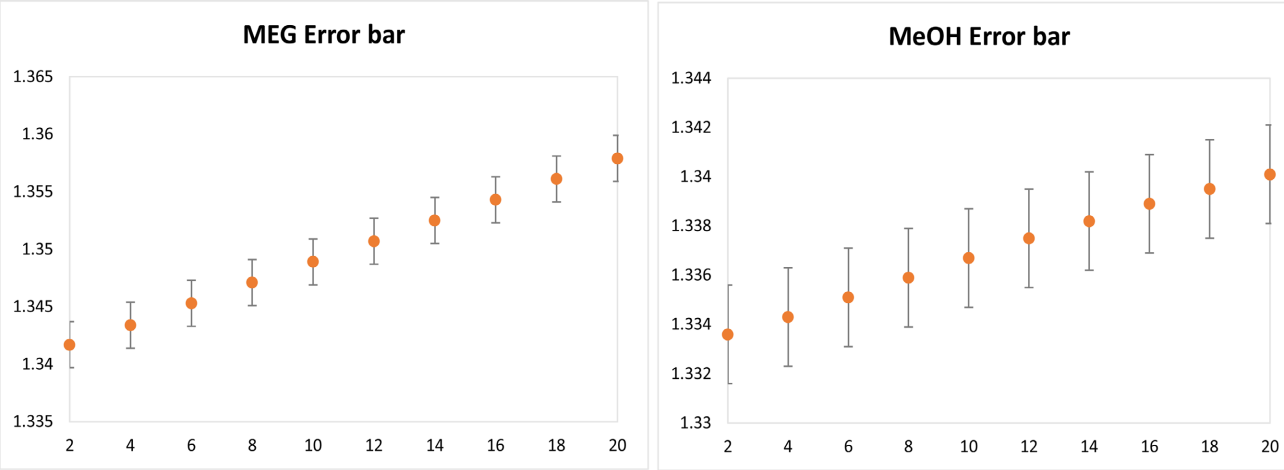

Figure 9. Calibration Error bar charts for MEG and MeOH.

Table 1. Regression summary of refractive index and weight percent relationship.

System	Regression Equation	Coefficient of Determination (R^2)
MEG System	Rd = 0.0009 C + 1.3394	0.9899
MeOH System	Rd = 0.0004 C + 1.3329	0.9976

their nature. The MeOH system has a relatively smaller slope of 0.0004, suggesting a moderate index rate rise with weight percent. The MEG system, on the other hand, has a steeper slope (0.0009), approximately twice that of MeOH, and indicates that it is denser, with stronger intermolecular interactions and a higher optical response per unit weight percent. These confirm a higher refractive sensitivity of MEG solutions' weight percent changes to MeOH solutions. This property demonstrates MEG's suitability for refractive-index-based weight percent process calibration and monitoring of hydrate-inhibition systems.

Refractive Index—Derived Weight percent for MEG and MeOH system

Refractive indices of Samples extracted from the loop, at target pressures of 135 psi, 130 psi 125 psi 120 psi and 115 psi, were measured at their extracted temperature. Table 2 showed the extracted temperature for each sample. The actual weight percentages of samples were derived from the refractive-index calibration equations established earlier (Table 1). The results (Figure 9) show that the actual concentration slightly decreases as operating pressure decreases from 135 psi to 115 psi. For example, the effective concentration of 10 wt% MEG solution was found to be equal to 9.56 wt% at a pressure of 135 psi, compared with a value of 8.44 wt% at the pressure of 115 psi. This effect can be attributed to a reduction of gas solubility at low pressure. A decrease in pressure facilitates the liberation of light gas constituents, which may strip some small quantity of water vapor, leaving the effective liquid phase composition modified. The measured refractive index values of MEG solutions extracted from the flow loop were converted into actual concentrations using the established calibration equation. Figure 9 shows that effective MEG concentration slightly decreases as operating pressure decreases

Table 2. Summary of extracted samples temperature.

Input wt%	115 psi		120 psi		125 psi		130 psi		135 psi	
	MEG (˚C)	MeOH (˚C)	MEG (˚C)	MeOH (˚C)	MEG (˚C)	MeOH (˚C)	MEG (˚C)	MeOH (˚C)	MEG (˚C)	MeOH (˚C)
2	17	16	18	17	18	17	19	19	21	20
4	16	15	18	16	18	15	18	17	19	19
6	16	14	17	15	17	14	17	16	17	17
8	14	13	16	14	16	13	16	15	16	16
10	13	12	15	12	14	12	15	14	15	15
12	13	11	14	11	14	11	14	14	15	14
14	12	10	13	11	13	10	14	13	14	14
16	11	9	13	10	12	9	14	12	13	13
18	10	9	12	10	12	9	13	12	13	12

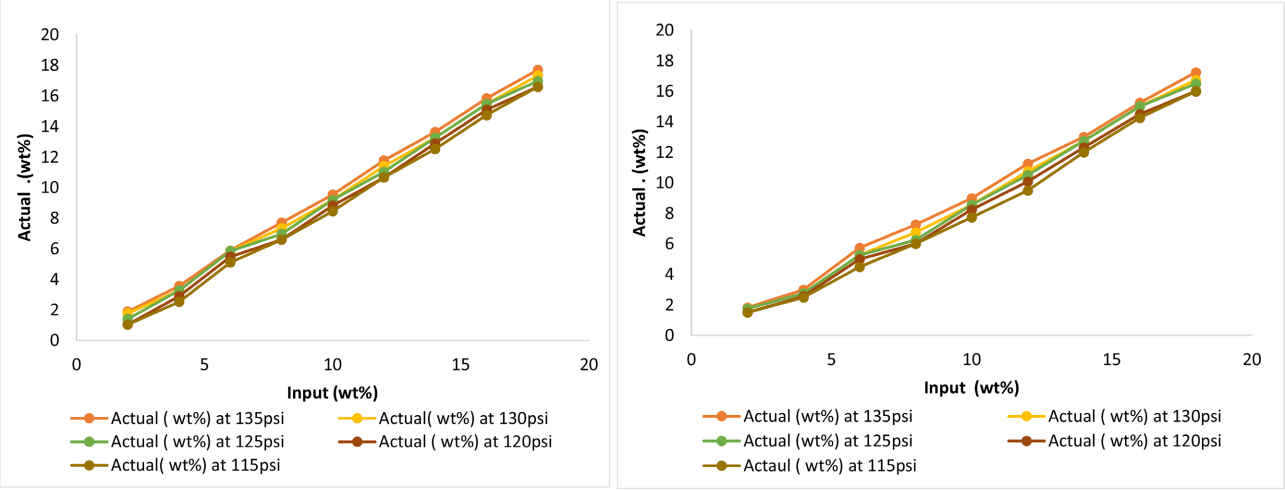

Figure 10. Relationship between input and actual weight percent of MEG and MeOH at varying operating pressure.

from 135 psi to 115 psi. At 135 psi, the actual concentrations closely match the input dosages, confirming minimal inhibitor loss to the non-aqueous phase under higher-pressure conditions. These results demonstrate that both inhibitors can sustain effective concentration even under pressure fluctuations typical of subsea pipelines. At a pressure of 135 psi, the actual concentrations are near the input values, thus demonstrating a steady state and low volatility of the inhibitor. But at lower pressure, the measured refractive index decreases slightly, therefore lowering the actual concentrations. For example, for the 10 wt% input from a 150 psi startup condition, the actual concentration for MEG was 9.56 wt% and 8.44 wt% at 135 psi and 115 psi, respectively, while MeOH was 9.0 wt% at 135 psi to about 7.75 wt% at 115 psi.

The higher decrease observed in MeOH could be explained by the higher volatility of methanol and lower hydrogen-bonding capacity in comparison with MEG.

As pressure decreases, gas solubility in the liquid phase diminishes, facilitating the migration of volatile components, particularly methanol, into the vapor phase compared to MEG, which remains more stable in the aqueous phase due to stronger intermolecular bonding [18] [21]. This explains why MeOH consistently exhibited greater concentration losses than MEG across the pressure range investigated.

The relationship between the input inhibitor volume and the actual volume available at a given operating pressure as shown in Figure 10, indicated that, the increase in input volume producing increase in the actual volume under all tested operating pressure. As seen in Figure 11, the loop pressure decreased with decreased temperature at a given input concentration, while an increase in input concentration decreased the temperature at a given pressure.

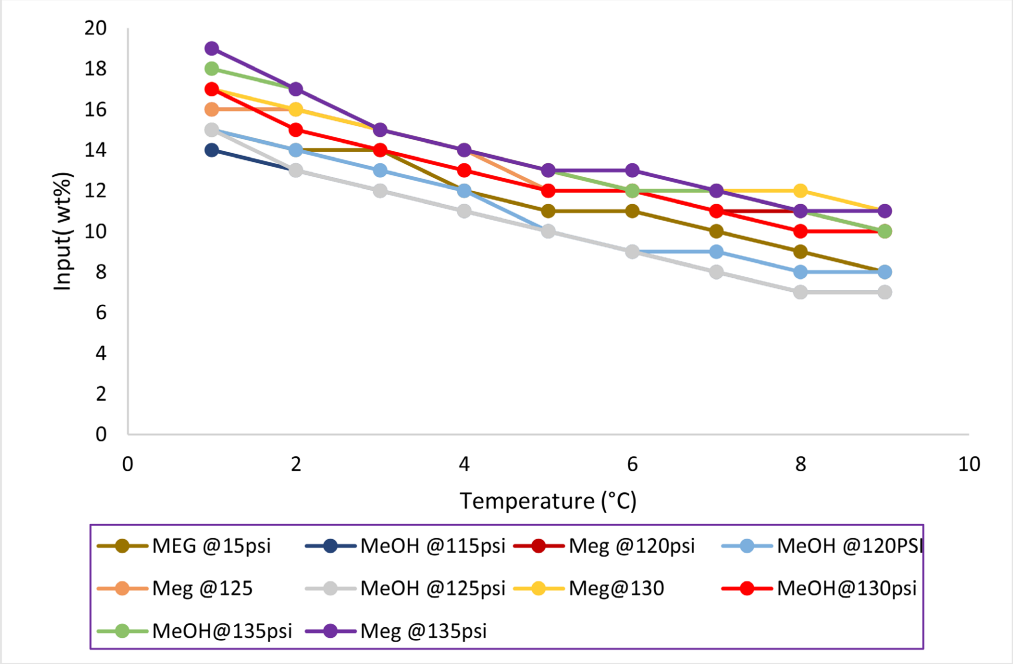

Figure 11. Input weight percent of MEG and MeOH at various pressures and temperatures.

Comparison of Actual and Input Inhibitor Weight Percent at Different Operating Pressures

At each experimental condition, the average difference between the actual and input weight percentages was evaluated. So, for a particular operating pressure, the actual weight obtained from all the tested input weight percent and their average deviation was calculated for both inhibitors. For example, at 135 psi, MEG retained approximately 96.2% of its input dosage, while MeOH retained 93.9%. As seen in Table 3, at 115 psi, retention dropped to 80.6% for MEG and 81.2% for MeOH, reflecting the increasing influence of volatility and gas-phase migration at lower pressures. These findings highlight that while both inhibitors are effective under high-pressure conditions, methanol's volatility poses a greater challenge for retention stability. MEG's stronger hydrogen-bonding interactions confer superior resilience, making it a more reliable inhibitor under fluctuating subsea pipe-

line pressures [28].

Overall, the results demonstrate that refractometry can accurately capture these pressure-dependent concentration variations, providing operators with a cost-effective and real-time tool for hydrate inhibitor optimization. By consistently interpreting concentration loss as a function of volatility-driven gas-phase partitioning, this study offers a clear mechanistic framework for understanding inhibitor behavior under variable operating conditions. Such insights are critical for optimizing dosage strategies, minimizing chemical waste, and ensuring effective flow assurance in offshore environments.

The primary limitation of this study is that the calibration curve was develop using water system only, Hence the presence of salt and or other existing contaminants in real field operation may introduce different effects that could possibly limit the accuracy and application of the model in the study.

Table 3. Pressure influence on the inhibitors' actual weight percent.

Pressure (psi)	Avg. Deviation (MEG) %	Avg. Deviation (MeOH) %	Retention Efficiency (MEG) %	Retention Efficiency (MeOH) %
135	3.8	6.1	96.2	93.9
130	7.3	10.4	92.7	89.6
125	10.3	11.8	89.7	88.2
120	16.3	15.3	83.7	84.7
115	19.4	18.8	80.6	81.2

5. Conclusions

1) Refractometry provides a sensitive and accurate method for monitoring MEG and MeOH concentrations ($R^2 > 0.98$), supporting its use for online hydrate inhibition control.

2) Established calibration equations allow conversion of refractive index measurements into actual inhibitor concentrations under varying pressures.

3) Both MEG and MeOH exhibit decreasing retention with lower operating pressures, with MEG showing slightly higher stability.

4) Accurate determination of actual inhibitor concentration enables operators to optimize dosage, reducing waste and ensuring effective hydrate prevention.

Overall, refractometry offers a fast, cost-effective, and reliable approach for hydrate inhibitor optimization in subsea pipeline operations.

Author Contributions

Mbooh T.R: Original draft, Investigation, Methodology, Conceptualization, Writing, Analysis, and Resources. Akhagbeme J. E: Analysis, Writing, Review, and Editing. Jeol O.F: Review and Supervision. Nwiabu N.D: Validation, Review and Supervision.

Conflicts of Interest

The authors declare no conflicts of interest regarding the publication of this paper.

References

[1] Kan, A.T., Fu, G., Watson, M.A. and Tomson, M.B. (2002) Effect of Hydrate Inhibitors on Oilfield Scale Formation and Inhibition. *International Symposium on Oilfield Scale*, Aberdeen, 30-31 January 2002, SPE-74657-MS. https://doi.org/10.2118/74657-ms

[2] Koh, C.A., Westacott, R.E., Zhang, W., Hirachand, K., Creek, J.L. and Soper, A.K. (2002) Mechanisms of Gas Hydrate Formation and Inhibition. *Fluid Phase Equilibria*, **194**, 143-151. https://doi.org/10.1016/s0378-3812(01)00660-4

[3] Linga, P., Daraboina, N., Ripmeester, J.A. and Englezos, P. (2012) Enhanced Rate of Gas Hydrate Formation in a Fixed Bed Column Filled with Sand Compared to a Stirred Vessel. *Chemical Engineering Science*, **68**, 617-623. https://doi.org/10.1016/j.ces.2011.10.030

[4] Sloan, E.D. (1998) Clathrate Hydrates of Natural Gases. 2nd Edition, Taylor & Francis.

[5] Circone, S., Kirby, S.H. and Stern, L.A. (2005) Direct Measurement of Methane Hydrate Composition along the Hydrate Equilibrium Boundary. *The Journal of Physical Chemistry B*, **109**, 9468-9475. https://doi.org/10.1021/jp0504874

[6] Carroll, J.J. (2009) Natural Gas Hydrates: A Guide for Engineers. 2nd Edition, Elsevier.

[7] Sloan, E.D. and Koh, C.A. (2007) Clathrate Hydrates of Natural Gas. 3rd Edition, CRC Press.

[8] Herath, D., Khan, F., Rathnayaka, S. and Rahman, M.A. (2015) Probabilistic Estimation of Hydrate Formation. *Journal of Petroleum Science and Engineering*, **135**, 32-38. https://doi.org/10.1016/j.petrol.2015.08.007

[9] Mokhatab, S., Wilkens, R.J. and Leontaritis, K.J. (2007) A Review of Strategies for Solving Gas-Hydrate Problems in Subsea Pipelines. *Energy Sources, Part A: Recovery, Utilization, and Environmental Effects*, **29**, 39-45. https://doi.org/10.1080/009083190933988

[10] Cheng, Y., Li, L., Mahmood, S. and Cui, Q. (2013) Fluid-Solid Coupling Model for Studying Wellbore Instability in Drilling of Gas Hydrate Bearing Sediments. *Applied Mathematics and Mechanics*, **34**, 1421-1432. https://doi.org/10.1007/s10483-013-1756-7

[11] Huang, T., Li, X., Zhang, Y., Wang, Y. and Chen, Z. (2020) Experimental Study of the Drilling Process in Hydrate-Bearing Sediments under Different Circulation Rates of Drilling Fluid. *Journal of Petroleum Science and Engineering*, **189**, Article ID: 107001. https://doi.org/10.1016/j.petrol.2020.107001

[12] Khan, M.S., Cornelius, B.B., Lal, B. and Bustam, M.A. (2018) Kinetic Assessment of Tetramethyl Ammonium Hydroxide (Ionic Liquid) for Carbon Dioxide, Methane and Binary Mix Gas Hydrates. In: Rahman, M.M., Eds., *Recent Advances in Ionic Liquids*, InTech. https://doi.org/10.5772/intechopen.77262

[13] Ledum, N.O., Osokogwu, U. and Okon, O.E. (2025) Evaluation of Local Hydrate Inhibitors in a Gas Dominated Flow Loop. *Petroleum & Coal*, **67**, 721-734. https://vurup.sk/storage/journal/4ebc2f75-9c5c-4d4e-91a7-4d0ddb060141.pdf

[14] Odutola, T.O., Onyekonwu, M.O. and Ikiensikimama, S.S. (2016). Effect of N-Vi-

nylcaprolactam on Hydrate Inhibition in Gas Dominated System. *SPE Nigeria Annual International Conference and Exhibition*, 2-4 August 2016, Lagos, SPE-184354-MS. https://doi.org/10.2118/184354-ms

[15] Okon, O.E., Ajienka, J.A., Ikeinsikimama, S.S., Elechi, V.U. and Odutola, T.O. (2018) Use of Locally Formulated Inhibitor from Agro Waste for Gas Hydrate Inhibition in a Mini Flow Loop. *International Journal of Science and Engineering Investigations*, **7**, 104-112.

[16] Akhagbeme, J.E., Ajienka, J.A., Wachikwu-Elechi, V.U. and Ikiensikimama, S.S. (2022) Gas Hydrate Formation and Dissociation: Effect of Salinity of Formation Water in Subsea Flowline. *SPE Nigeria Annual International Conference and Exhibition*, 1-3 August 2022, Lagos, SPE-212011-MS. https://doi.org/10.2118/212011-ms

[17] Samimi, A. (2012) Offer a New Model to Prevent Formation of Hydrate in Gas Pipeline in Gas Refinery. *International Journal of Innovation and Applied Studies*, 1, 226-231. https://ijias.issr-journals.org/abstract.php?article=IJIAS-12-326-02

[18] Aminnaji, M., Tohidi, B., Burgass, R. and Atilhan, M. (2017) Effect of Injected Chemical Density on Hydrate Blockage Removal in Vertical Pipes: Use of MEG/MeOH Mixture to Remove Hydrate Blockage. *Journal of Natural Gas Science and Engineering*, **45**, 840-847. https://doi.org/10.1016/j.jngse.2017.06.030

[19] Kartnaller, V., Venâncio, F., Cajaiba, J. and Rosário, F.D. (2017) Study of the Effect of Monoethylene Glycol MEG on the Precipitation of Calcium Carbonate in a Pressurized Dynamic System. *OTC Brasil*, Rio de Janeiro, 24-26 October 2017, OTC-28111-MS. https://doi.org/10.4043/28111-ms

[20] Saberi, A., Alamdari, A., Shariati, A. and Mohammadi, A.H. (2018) Experimental Measurement and Thermodynamic Modeling of Equilibrium Condition for Natural Gas Hydrate in MEG Aqueous Solution. *Fluid Phase Equilibria*, **459**, 110-118. https://doi.org/10.1016/j.fluid.2017.11.034

[21] Brustad, S., Løken, K.P. and Waalmann, J.G. (2005) Hydrate Prevention Using MEG Instead of Meoh: Impact of Experience from Major Norwegian Developments on Technology Selection for Injection and Recovery of Meg. *Offshore Technology Conference*, Houston, 2-5 May 2005, OTC-17355-MS. https://doi.org/10.4043/17355-ms

[22] Elechi, V.U., Ikiensikimama, S.S., Ajienka, J.A., Akaranta, O., Onyekonwu, M.O., Odutola, T.O. and Okon, O.E. (2018) Gas Hydrate Inhibition in a Simulated Off-Shore Environment Using Local Inhibitor. *Nigeria Annual International Conference and Exhibition*, Lagos, 6-8 August 2018, SPE-193439-MS.

[23] Gao, S. (2009) Hydrate Risk Management at High Watercuts with Anti-Agglomerant Hydrate Inhibitors. *Energy & Fuels*, **23**, 2118-2121. https://doi.org/10.1021/ef8009876

[24] May, E.F., Lim, V.W., Metaxas, P.J., Du, J., Stanwix, P.L., Rowland, D., *et al.* (2018) Gas Hydrate Formation Probability Distributions: The Effect of Shear and Comparisons with Nucleation Theory. *Langmuir*, **34**, 3186-3196. https://doi.org/10.1021/acs.langmuir.7b03901

[25] Ahmed, M. and Sahweity, S. (2020) Hydrate Management Controls in Saudi Aramco's Largest Offshore Non-Associated Gas Fields. *Offshore Technology Conference*, Houston, 4-7 May 2020, OTC-30768-MS.

[26] Swanson, T.A., Petrie, M. and Sifferman, T.R. (2005) The Successful Use of Both Kinetic Hydrate and Paraffin Inhibitors Together in a Deepwater Pipeline with a High Water Cut in the Gulf of Mexico. *SPE International Symposium on Oilfield Chemistry*, The Woodlands, 2-4 February 2005, SPE-93158-MS. https://doi.org/10.2118/93158-ms

[27] Phan, A., Bui, T., Acosta, E., Krishnamurthy, P. and Striolo, A. (2016) Molecular Mechanisms Responsible for Hydrate Anti-Agglomerant Performance. *Physical Chemistry Chemical Physics*, **18**, 24859-24871. https://doi.org/10.1039/c6cp03296f

[28] Bellucci, M.A., Walsh, M.R. and Trout, B.L. (2018) Molecular Dynamics Analysis of Anti-Agglomerant Surface Adsorption in Natural Gas Hydrates. *The Journal of Physical Chemistry C*, **122**, 2673-2683. https://doi.org/10.1021/acs.jpcc.7b09573

[29] AlHarooni, K., Barifcani, A., Pack, D., Gubner, R. and Ghodkay, V. (2015) Inhibition Effects of Thermally Degraded MEG on Hydrate Formation for Gas Systems. *Journal of Petroleum Science and Engineering*, **135**, 608-617. https://doi.org/10.1016/j.petrol.2015.10.001

[30] Okereke, N.U., Edet, P.E., Baba, Y.D., Izuwa, N.C., Kanshio, S. and Nwogu, O. (2018) An Assessment of Hydrate Inhibition in Deep-Water Production System Using Low-Dosage Hydrate Inhibitor and Mono Ethylene Glycol. *Journal of Petroleum Exploration and Production Technology*, **10**, 1169-1182.

[31] Lavallie, O., AL Ansari, A., O'Neill, S., Chazelas, O., Glenat, P. and Tohidi, B. (2009) Successful Field Application of an Inhibitor Concentration Detection System in Optimising the Kinetic Hydrate Inhibitor (KHI) Injection Rates and Reducing the Risks Associated with Hydrate Blockage. *International Petroleum Technology Conference*, Doha, 7-9 December 2009, IPTC-13765-MS. https://doi.org/10.2523/iptc-13765-ms

[32] Tohidi, B., Chapoy, A., Yang, J., Ahmadloo, F., Valko, I. and Zain, Z.M. (2008) Developing Hydrate Monitoring and Early Warning Systems. *Offshore Technology Conference*, Houston, 5-8 May 2008, OTC-19247-MS. https://doi.org/10.4043/19247-ms

[33] Mazloum, S., Yang, J., Chapoy, A. and Tohidi, B. (2011) A Novel Technique for Optimizing Hydrate Inhibitor Injection Rate. *OTC Brasil*, Rio de Janeiro, 4-6 October 2011, OTC-22487-MS. https://doi.org/10.4043/22487-ms

[34] Yang, J.H., Chapoy, A., Mazloum, S. and Tohidi, B. (2011) Development of a Hydrate Inhibition Monitoring System by Integration of Acoustic Velocity and Electrical Conductivity Measurements. *Exploration and Production*: *The Oil and Gas Review*, **9**, 36-40. https://www.hydrafact.com/wp-content/uploads/2024/06/HydraCHEK-Oil-Gas-Review.pdf

[35] Mazloum, S., Chapoy, A., Yang, J. and Tohidi, B. (2011) A Simple Correlation for Calculating the Hydrate Suppression Temperature Based on Water Activity. 7*th International Conference on Gas Hydrates*, Edinburgh, 17-21 July 2011.

[36] Seo, Y., Kang, S. and Jang, W. (2009) Structure and Composition Analysis of Natural Gas Hydrates: ^{13}C NMR Spectroscopic and Gas Uptake Measurements of Mixed Gas Hydrates. *The Journal of Physical Chemistry A*, **113**, 9641-9649. https://doi.org/10.1021/jp904994s

[37] K. Haghi, R., Yang, J. and Tohidi, B. (2018) Integrated near Infrared and Ultraviolet Spectroscopy Techniques for Determination of Hydrate Inhibitors in the Presence of NaCl. *Industrial & Engineering Chemistry Research*, **57**, 11728-11737. https://doi.org/10.1021/acs.iecr.8b02372

[38] Antony, A. and Mitra, J. (2018) Refractive Index-Assisted UV/Vis Spectrophotometry to Overcome Spectral Interference by Impurities. *Analytica Chimica Acta*, **1149**, Article ID: 238186.

[39] Worsfold, P., Townshend, A. and Poole, L. (2004) Encyclopedia of Analytical Science. 2nd Edition, Elsevier.

[40] Zhang, Z.W., Yin, W.F., Wen, T.D., *et al.* (2009) Study of the Relational Expression

of Solution Concentration and Its Refractive Index. *Journal of North University of China Natural Science Edition*, **30**, 281-285. (In Chinese)

[41] Musa, R.R., Adnan, S.A. and Hammadi, A.M. (2017) Design & Fabrication of Evanescent Wave Fiber Optic Sensor. *Advances in Natural & Applied Sciences*, **11**, 130-139.

[42] Odutola, T.O., Ajienka, J.A., Onyekonwu, M.O. and Ikiensikimama, S.S. (2017) Design, Fabrication and Validation of a Laboratory Flow Loop for Hydrate Studies. *American Journal of Chemical Engineering*, **5**, 28-41.

Appendix

A1. Relationship between Input and Actual Weight percent of MEG and MeOH at 135 and 130 psi.

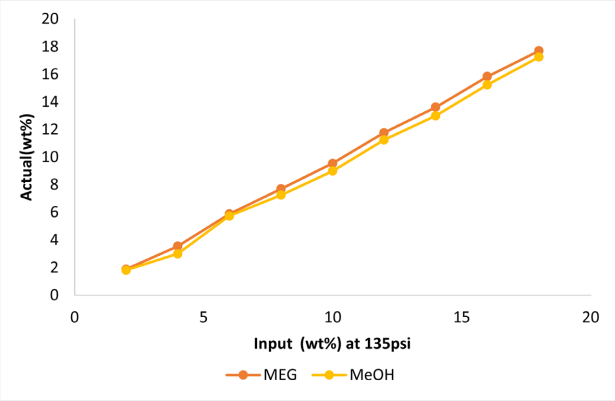

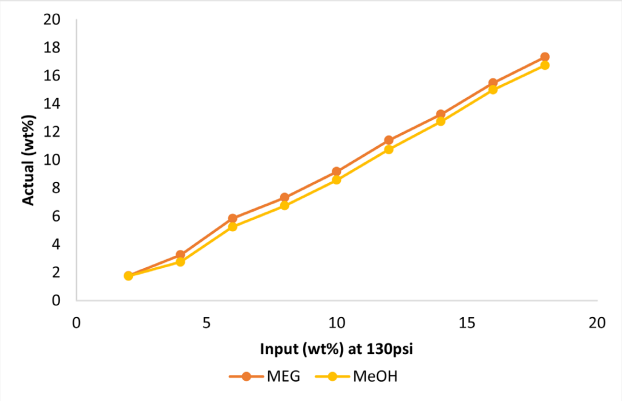

A2. Relationship between Input and Actual Weight Percent of MEG and MeOH at 125 and 120 psi

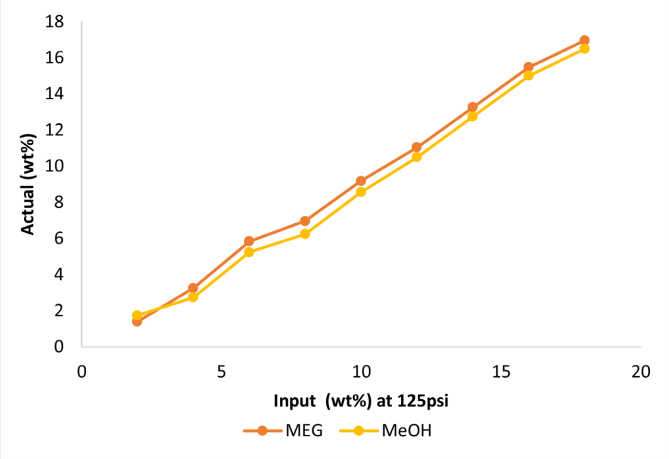

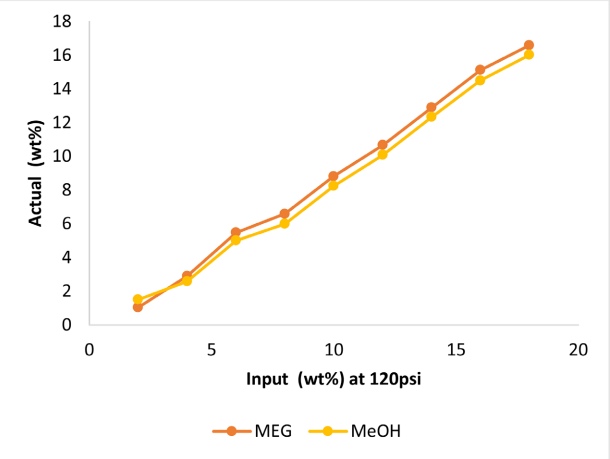

A3. Relationship between Input and Actual Weight Percent of MEG and MeOH at 115

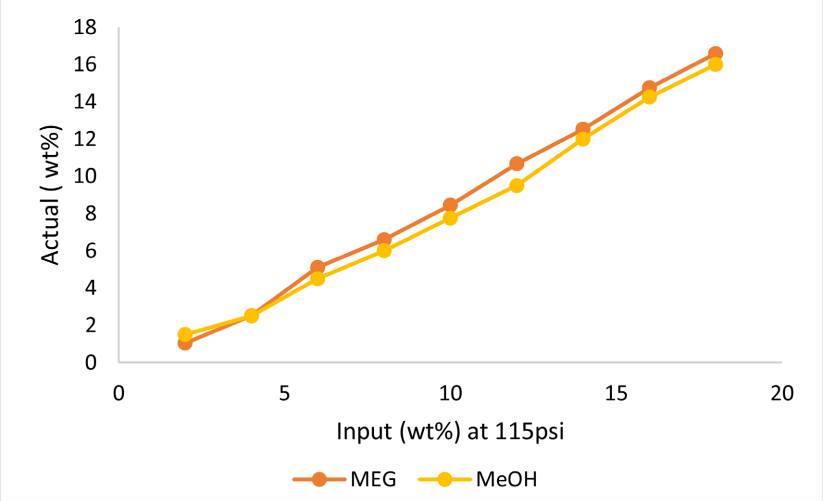

A4. Calibration Reading*

Weight Percent	Refractive Index MEG				Refractive Index MeOH			
	First reading	Second reading	Third reading	Average reading	First reading	Second reading	Third reading	Average reading
2	1.3417	1.3418	1.3417	1.3417	1.3336	1.3336	1.3337	1.3336
4	1.3434	1.3434	1.3435	1.3434	1.3343	1.3343	1.3343	1.3343
6	1.3454	1.3453	1.3453	1.3453	1.3351	1.3352	1.3351	1.3351
8	1.3471	1.3472	1.3471	1.3471	1.3359	1.3359	1.3360	1.3359
10	1.3489	1.3489	1.349	1.3489	1.3368	1.3367	1.3367	1.3367
12	1.3507	1.3507	1.3507	1.3507	1.3375	1.3375	1.3375	1.3375
14	1.3525	1.3526	1.3525	1.3525	1.3382	1.3382	1.3383	1.3382
16	1.3543	1.3543	1.3544	1.3543	1.3389	1.3389	1.3389	1.3389
18	1.3562	1.3561	1.3561	1.3561	1.3395	1.3396	1.3395	1.3395
20	1.3579	1.3580	1.3579	1.3579	1.3401	1.3401	1.3401	1.3401